LABORATOIRE ASSOCIE A L'IN2P3

institut de physique nucléaire

IPNO-DRE-86-18

SPONTANEOUS EMISSION OF FRAGMENTS FROM NUCLEI

E. Hourani

SPONTANEOUS EMISSION OF FRAGMENTS FROM NUCLEI

E. HOURANI

Institut de Physique Nucléaire, BP n° 1
91406 ORSAY Cédex, France

1 - INTRODUCTION

The spontaneous emission of fragments from nuclei is a recently discovered radioactivity. Essentially, the discovery was that some radioactive α-sources like Ra and U isotopes are emitters of fragments like ^{14}C, $^{24,25}Ne$, ... with branching ratios of 10^{-10} or less relative to the α-particles.

The theoretical prediction of this radioactivity was published in 1980 by Sandulescu, Poenaru and Greiner[1].

The measurement which established this radioactivity was published in 1984 by Rose and Jones who reported the emission of ^{14}C nuclei from ^{223}Ra with a branching ratio of $(8.5 \pm 2.5) \times 10^{-10}$ relative to α-particles[2].

Within a few months following the publication of Rose and Jones several groups from different laboratories using various techniques confirmed their result[3-6]. The search for other new cases of ^{14}C radioactivity was the logical next step. Such cases were found in other isotopes of radium, i.e. $^{222,224}Ra$[5] and ^{226}Ra[7-8]. Further effort yielded the discovery of Ne emission from ^{232}U[9], ^{233}U[11], ^{231}Pa[10] and ^{230}Th[12].

During their pioneering work, Rose and Jones met a serious difficulty in the choice of the decay to investigate because they were guided only by Q-value and Gamow factor considerations. The following investigators were oriented efficiently by the realistic predictions of Poenaru et al.[13] obtained, thereafter, by normalization to the result of Rose and Jones. The difficulties encountered by these investigators originated, mainly, in the preparation of intense radioactive sources and in the setup of selective detection techniques.

At present, the status in the spontaneous fragment emission study resembles many other advanced fields in nuclear physics : very specialized techniques are needed to add new experimental results and theoretical model refinements are being established in order to take into account the overall features of the experimental results.

We found it convenient to classify the experimental results obtained so far according to the different detection techniques. Thus, after a section for basic considerations, we devote three sections to describe the experiments corresponding to three detection techniques, i.e. the $\Delta E \times E$ telescope, the magnetic spectrometers and the track recording foils. In a last section we present a general discussion.

2 - BASIC CONSIDERATIONS

The decay of a nucleus (Z, A) of mass $M(Z, A)$ into a fragment (z, a) and a residual nucleus $(Z-z, A-a)$ is energetically characterized by the Q-value defined by :

$$Q = M(Z, A) - M(z, a) - M(Z-z, A-a)$$

The decay is possible only when $Q > 0$. Using a table of masses, one can see that Q is positive for a large number of heavy nuclei decaying into several types of fragments and that the largest Q-values are obtained in the decays where the residual nucleus is the doubly magic nucleus ^{208}Pb or a neighboring nucleus. The kinetic energy of the emitted fragment is deduced from Q by $Q \times (A-a)/A$. In addition, the main characteristic of the decay, which is the decay rate, is very sensitive to Q.

The simplest way to evaluate the decay rate is the traditional α-model where the fragment is supposed to be preformed inside the nucleus and impinging on a confining Coulomb barrier. The tunneling probability across the barrier, also called Gamow factor, is given, within the WKB approximation by :

$$G = \exp \left[-2 \int_a^b dr \, (2\mu(U(r) - Q) / \hbar^2)^{1/2} \right]$$

where $U(r) = z(Z-z)e^2/r$, $a = r_0 \times ((A-a)^{1/3} + a^{1/3})$, μ is the reduced mass and b is defined by $U(b) = Q$.

We calculated the fragment/α Gamow factor ratios for the most probable decays of the members of the ^{235}U natural series. We present, in table 1, their values for $r_0 = 1.15$ and 1.20. These Gamow factor ratios show the high sensitivity of the tunneling to the values of Q and r_0. On the other hand, they correctly select for a given parent the most probable decay. Also, they are meaningful to compare the probabilities of the decays of two neighboring parents. Unfortunately, they completely fail to predict either a realistic value for a given decay or the ratio of the decays of two parents as far from each other as ^{223}Ra and ^{235}U.

TABLE 1 : Most probable decays in the ^{235}U natural series

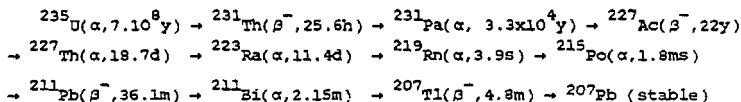| DECAY	Q-Value (MeV)	FRAGMENT/α			
		Gamow factor ratio		Branching ratio	
		$r_o = 1.15$	$r_o = 1.20$	ref.13	ref.14
$^{235}U \rightarrow \, ^{28}Mg + \, ^{207}Th$	72.20	3.3×10^{-3}	1.14	1.6×10^{-11}	1.47×10^{-16}
$^{231}Pa \rightarrow \, ^{24}Ne + \, ^{207}Tl$	60.42	2.9×10^{-3}	0.37	1.0×10^{-10}	9.4×10^{-12}
$^{227}Th \rightarrow \, ^{14}C + \, ^{213}Po$	29.45	5.3×10^{-12}	9.2×10^{-11}	4.0×10^{-16}	9.2×10^{-17}
$\rightarrow \, ^{18}O + \, ^{209}Pb$	44.21	2.1×10^{-10}	9.8×10^{-9}	5.0×10^{-16}	7.3×10^{-18}
$^{223}Ra \rightarrow \, ^{12}C + \, ^{211}Pb$	27.73	6.9×10^{-12}	8.9×10^{-11}	4.0×10^{-15}	7.4×10^{-19}
$\rightarrow \, ^{13}C + \, ^{210}Pb$	28.85	1.3×10^{-10}	1.9×10^{-9}	4.0×10^{-14}	1.1×10^{-15}
$\rightarrow \, ^{14}C + \, ^{209}Pb$	31.84	1.2×10^{-5}	1.7×10^{-4}	3.2×10^{-9}	6.5×10^{-9}
$^{219}Rn \rightarrow \, ^{14}C + \, ^{205}Hg$	28.11	2.6×10^{-16}	4.3×10^{-15}	6.3×10^{-21}	5.7×10^{-21}

At present, it is the fissionlike description, even in its simplified form as was given by Poenaru et al.[13] and, later on, by Yi-Jin Shi and Swiatecki[14], which yields the best predictions for the spontaneous emission of fragments. Such a description takes into account the nuclear collective oscillations times the fragment penetrability factor through a deformation energy barrier parametrized to fit experimental data. In table 1, are presented the fragment/α branching ratios calculated with these supersymmetric fission models for the decays already selected according to Gamow factor ratios. Not only do the calculated branching ratios select ^{223}Ra as the best fragment emitter candidate but also they predict realistic values when compared to observed results.

3 - THE ^{14}C   RADIOACTIVITY OF ^{223}Ra MEASURED WITH A ΔExE TELESCOPE

A ΔExE Si surface barrier detector telescope was used by Rose and Jones[2] in their discovery for the ^{14}C decay of ^{223}Ra and later on by Alexandrov et al. [4] in their repetition of the measurement of Rose and Jones. With this technique the telescope is placed in direct view of the source. In the experiment of Rose and Jones, the ΔE detector was 8.2 μm thick with an area of 200mm^2, the E detector had an area of 300 mm^2 and the solid angle ΔΩ was 1/3sr, whereas in the experiment of Alexandrov et al. the detectors were 16 μm and 500 μm thick with ΔΩ = 0.1 sr.

Since the high counting rate of α-particles producing multiple pile-up events is the most severe constraint in a ΔExE telescope measurement, the source and the measurement time should be carefully chosen.

The main decay sequence of ^{235}U is :

$$^{235}\text{U}(\alpha,7.10^8\text{y}) \rightarrow {}^{231}\text{Th}(\beta^-,25.6\text{h}) \rightarrow {}^{231}\text{Pa}(\alpha, 3.3\text{x}10^4\text{y}) \rightarrow {}^{227}\text{Ac}(\beta^-,22\text{y})$$
$$\rightarrow {}^{227}\text{Th}(\alpha,18.7\text{d}) \rightarrow {}^{223}\text{Ra}(\alpha,11.4\text{d}) \rightarrow {}^{219}\text{Rn}(\alpha,3.9\text{s}) \rightarrow {}^{215}\text{Po}(\alpha,1.8\text{ms})$$
$$\rightarrow {}^{211}\text{Pb}(\beta^-,36.1\text{m}) \rightarrow {}^{211}\text{Bi}(\alpha,2.15\text{m}) \rightarrow {}^{207}\text{Tl}(\beta^-,4.8\text{m}) \rightarrow {}^{207}\text{Pb (stable)}$$

Examining this sequence one sees, effectively, that ^{227}Ac is the most convenient precursor for ^{223}Ra with regard to its half-life of 22 y and to a measurement time of several months.

In the experiment of Rose and Jones, the Ac source had an activity of 3.3 μCi in α-particles giving a counting rate of ≈ 4000c/s and producing up to quadruple pile-up, whereas in the experiment of Alexandrov et al. an Ac source of ≈ 85 μCi yielded a counting rate of 25 000 c/s and produced up to quintuple pile-up. Figure 1 shows the results of Rose and Jones obtained in a run of 189 days. In this figure, 11 events lie around a value of 30 MeV of the total energy which corresponds to the energy (deduced from the Q-value) of the ^{14}C nuclei expected to be emitted by ^{223}Ra, whereas their ΔE fall inside the two dashed lines delimiting the location of C isotopes as extrapolated from a calibration with an α-source. In figure 2, we show the results of Alexandrov et al. obtained in a measurement of 30 days. There are 7 events lying around the total energy of the expected ^{14}C nuclei (indicated by an arrow) and within the location of C isotopes (limited by dashed lines).

Here the arrow and the dashed lines represent the calibration established with a ^{12}C beam from the cyclotron of the Kurchatov Institute of Atomic Energy.
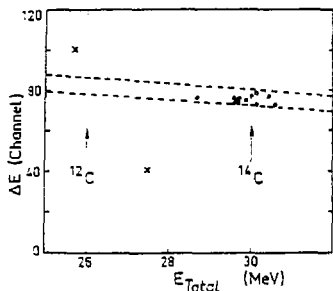

Fig. 1 Results of Rose and Jones[2] with an ^{227}Ac source and a ΔExE telescope. In dots, the ^{14}C nuclei emitted by ^{223}Ra. The arrows and the dashed lines are the results of the calibration. The lower of the two crosses represents a quadruple pile-up. The upper cross is an event which was recorded during a thunderstorm.
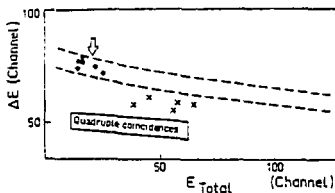
Fig. 2 Results of Alexandrov et al.[4] with an ^{227}Ac source and a ΔExE telescope. In dots, the ^{14}C nuclei emitted by ^{223}Ra. The arrow and the dashed lines are the results of the calibration. The solid lines bound the region of quadruple coïncidences of α pulses. The crosses represent quintuple coïncidences.

On the basis of the location of the 11 events in the ΔExE plot (fig. 1) and of a favorable calculated Gamow factor (table 1) Rose and Jones established the ^{14}C decay of ^{223}Ra. As to the results of Alexandrov et al., they showed that the measurement of Rose and Jones was reproducible.

Considering the ΔExE telescope technique itself, we see that it involves here the detection of the very high flux of α-particles emitted by the sources, a fact which not only produces a high rate of multiple pile-up events even in long measurements but also damages the detectors. These features led physicists to use in the later experiments on spontaneous fragment emission more selective techniques, i.e. the magnetic spectrometers and the track detectors.

4 - EXPERIMENTS ON ^{14}C DECAY OF Ra ISOTOPES WITH MAGNETIC SPECTROMETERS

Because the decay into fragments occurs as very low branching ratio relative to α-emission in an α-source, an attractive idea is to select the fragments from the very high flux of α-particles and to direct them towards a detector. This is accomplished by magnetic spectrometers. The main advantage in such a method is to use very strong sources with no risk of damaging the detectors. The limitation in the performances originates in the smallness of the solid angle of the existing spectrometers and the acceptable thicknesses of the sources which do not disturb too much the kinetic energies of the emitted fragments. Many spectrometers were certainly considered but only two led to diffused publications : the superconducting solenoïdal coil SOLENO[15] at Orsay and the well-known type Enge split-pole of Argonne. The main characteristics of these devices will be succintly described and the experimental results will be given.

4.1 - Experiments with SOLENO

The spectrometer SOLENO is a superconducting solenoidal coil surrounded by an iron shield and envelopping a vacuum chamber. It presents a perfect azimutal symmetry with a large solid angle of 100 msr and a large bandwidth in Bρ of 5%, which seem to be the suitable characteristics for fragment selection. When the electric current of SOLENO is set to focus the fragments emitted from the source on the detector, the doubly charged α-particles, $α^{++}$, emitted by the source are focussed well before the detector and the singly charged $α^+$ are focussed well behind the detector[3]. So both of them do not impinge on the detector (fig. 3a). The transmission of SOLENO is usually described in terms of the effective solid angle at its entrance versus the magnetic rigidity Bρ of the incident ions (fig. 3b). When the ions have a well-defined energy, e.g. in case of thin sources, the focussing is adjusted in order to place the representative point of these ions at the maximum of the transmission curve, whereas when the ions have a wide distribution of energy, e.g. in case of thick sources, their representative points lie along the whole transmission curve. In the later case, it results in a reduced effective solid angle.
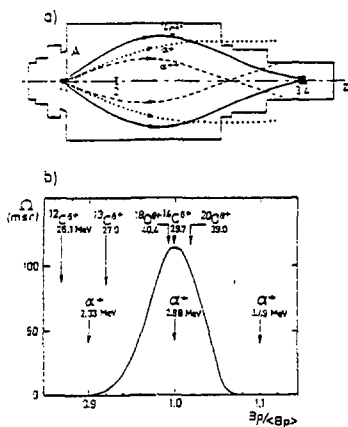
Fig. 3 (a) Setup inside the vacuum chamber of SOLENO : 1 – source, 2 – baffle, 3,4 – ΔExE telescope. The trajectories of focussed $^{14}C^{6+}$ and unfocussed α^+ and α^{++} are shown. (b) Transmission curve of SOLENO established with an α-source. The arrows indicate the positions of degraded α^+ and of different fragments which could be emitted from the daughters of ^{227}Ac. From reference 3.
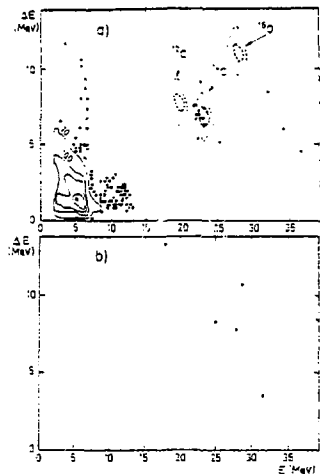
Fig. 4 Results of Galès et al.[3] with an ^{227}Ac source and a ΔExE telescope placed in the focussing plane of SOLENO. (a) In dashed lines are the results of the calibration. A group of events falls inside the expected location of ^{14}C nuclei emitted by ^{223}Ra. At low energy counts due to α-particles. (b) Background measurement where a slight contamination from Cf source was revealed.

The detection system consisted of a ΔExE telescope of silicon surface barrier detectors. The dimensions of the ΔE and E detectors were 9 μm x 200 mm^2 and 200 μm x 300 mm^2 respectively.

The telescope was calibrated with a ^{14}C beam from the Tandem of Orsay.

Despite the high magnetic rejection of SOLENO for the α-particles emitted by the sources there were two categories of α which could reach the detectors :

a) the α particles emitted by the Rn and its daughters deposited around the detectors (the Rn as a gas emanates from the source and travels inside the vacuum towards the detection area).

b) the degraded α^+ particles, especially in case of thick sources, which fall inside
ıe transmission band of SOLENO.

However, all the detected α are represented near the origin in the $\Delta E \times E$ plane.
)nly multiple pile-up could give events extending to the ^{14}C location.

In figure 4a, we show the results[3] of a run of 5 days with a source of ^{227}Ac of 210
ıCi in ^{223}Ra. The presence of a group of 11 events in the middle of the figure and inside
:he location of the expected ^{14}C nuclei (given by dotted line') has unambiguously
confirmed the ^{14}C decay of ^{223}Ra discovered by Rose and Jones. In figure 4a, the counts
at the left originate in α-particles and the six dispersed events observed at the right are due
to a slight contamination by a Cf source during a preliminary test (revealed in the
background measurement of figure 4b).

In figure 5, are shown the results[7] of the ^{14}C decay of ^{222}Ra, characterized by a
striking clarity, which have confirmed the results of Price et al.[5] performed with track
detectors.

In figure 6, are shown the results[7] which have proven the ^{14}C decay of ^{226}Ra.
Four events, labelled from 1 to 4 and located around the ^{14}C line characterizing a thick
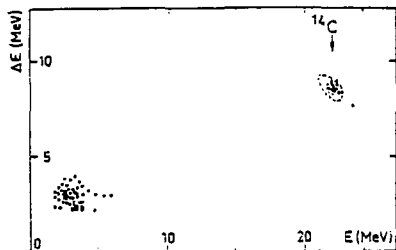source emission, were identified as ^{14}C nuclei emitted by the ^{226}Ra source.

Fig. 5   Results of Hourani et al.[7] with a ^{230}U
source and a $\Delta E \times E$ telescope placed in the focussing
plane of SOLENO. A group of events coïncide with
the location of the ^{14}C fragments expected from the
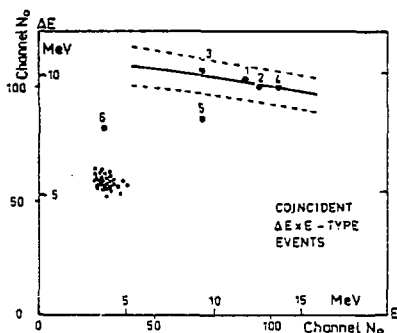daughter ^{222}Ra. Events at low energy are due to α-
particles.

Fig. 6   Results of Hourani et al.[7] with a ^{226}Ra
source and a $\Delta E \times E$ telescope placed in the focussing
plane of SOLENO. Events labelled from 1 to 4 fall
within the location of ^{14}C given by dashed lines.
They are ^{14}C fragments emitted by ^{226}Ra. Other
events are due to α-particles.

Finally, it is worthwhile to mention other capabilities of SOLENO :

- Taking into account the small size ($\phi < 16$ mm) and the reduced thickness ($<$ 1mg/cm^2) required for the source, fragment/α branching ratios of 10^{-13} or better could be attained for sources of half-lives shorter than ten years.

- Precise energy measurement or mass identification are possible, especially when the version of SOLENO with two coils is used.

4.2 - Experiment with an Enge split-pole magnetic spectrograph

Kutschera et al.[6] measured the energy and the mass of the C nuclei emitted in the decay of ^{223}Ra. A strong ^{227}Th source containing ^{223}Ra as a daughter was used and an Enge split-pole magnetic spectrograph with a gaseous detector in its focal plane served to select and to detect the C nuclei.

The source of ^{227}Th, 100μg/cm^2 thick, with a diameter of 5mm, had an average activity of 9.2 mCi in ^{223}Ra. The spectrograph had a solid angle of 4.38 x 10^{-4} of 4 π and it accepted ^{14}C^{6+} ions with energies ranging from 20 to 33 MeV.

The detector measured for each focussed ion its magnetic rigidity $\beta\rho$ (deduced from a position measurement in the focal plane), its specific energy loss ΔE and its total energy E.

A measurement of 6.09 days with the ^{227}Th source was performed. The counting rate was of about 700c/s due to the same origins as explained with the spectrometer SOLENO. A background measurement of 2.85 days was obtained by turning the source holder by 180°. The comparison of the two measurements, in either ΔExE or $Ex\beta\rho$ plane, yielded a total of 24 events falling outside the background region and at the ^{14}C location as obtained with a calibration using a ^{14}C beam from the Tandem of Argonne.

There was a considerable spread in ΔE measurement resulting from the dependence of the path lengths across the ΔE detector on the angular incidence at the entrance of the spectrograph. The total energy signal was better carried out and there was essentially no deterioration in the $\beta\rho$ signal. Therefore we present, in figure 7, the 24 events plotted in the $Ex\beta\rho$ plane. The large part of the events clearly falls on the ^{14}C^{6+} mass line. Three of them fall on a different line which is consistent with the location of ^{14}C^{5+}.

There is no doubt the results of this experiment demonstrated that the detected ions had a mass number 14. Unfortunately the statistics of the data and the energy resolution were not sufficient to allow either the identification of possible transition to excited states in ^{209}Pb (as was attempted by the authors in figure 8) or the existence of a parallel decay of ^{223}Ra by ^{13}C emission (suggested by the occurrence of one event on the ^{13}C mass line in figure 7).
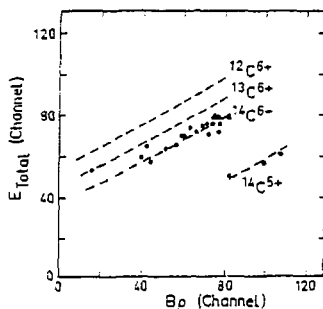

Fig. 7 Results of Kutschera et al. [6] with an ^{227}Ac source and a gaseous detector placed in the focal plane of a split-pole spectrograph. The events coincide with the location of ^{14}C nuclei as given in dashed lines by the calibration.
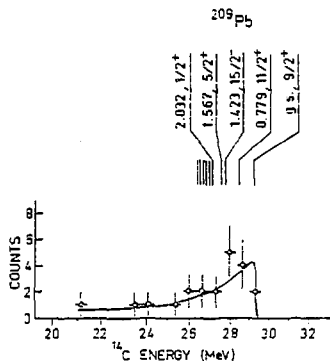
Fig. 8 The events shown in figure 7 are plotted here versus the total energy. The positions of the g.s. and of some excited states of the daughter ^{209}Pb are indicated.

5. EXPERIMENTS WITH TRACK DETECTORS

Track detectors are insulating solids where paths of heavily ionizing particles may be made visible in a microscope after a chemical etching [16]. Polycarbonate detectors have been used so far in the detection of fragments. Tuffak foils which are sensitive to particles with $Z > 2$ were used by Price et al. [5] to measure the charge number and the range of C nuclei. A maximum α-dose of $6.10^{10}\alpha/cm^2$ was tolerated in order to control the degree of overlapping of short tracks of C or O ions produced as recoil nuclei in elastic collisions with α-particles inside the polycarbonate. Much less sensitive polycarbonate, i.e. the polyethylene terephthalate, also called cronar, was used thereafter by different authors to detect Ne fragments [9-12]. This detector is sensitive to ions with $Z > 6$ and the limiting α-dose is about $2.10^{11}\alpha/cm^2$.

5.1 - Experiments on Ra isotopes

Price et al.[5] selected radium and francium isotopes produced in spallation reaction at the CERN synchrocyclotron using the ISOLDE facility. The ions of masses 221-224 were implanted in the bases of cups on the top and sides of which were deployed a 125μm Tuffak sheet covered with a 10μm Makrofol sheet (fig. 9).
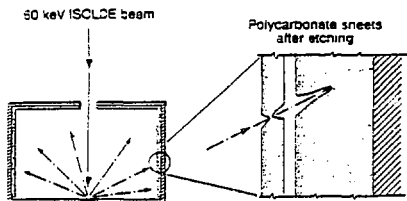

Fig. 9 Radium isotope collector cup used in the experiment of Price et al.[5] where polycarbonate sheets were taken as track detectors.

In figure 10, they plotted the rate of the chemical etching along the track against the residual range. Because the etching rate along the track depends on the primary ionization rate, which is a function of the velocity and the charge number Z of the particle, this plot has the property of a $\Delta E \times E$ detector telescope with respect to the identification in Z. In figure 10, measurements at two points along the tracks of ^{14}C emitted from ^{223}Ra are
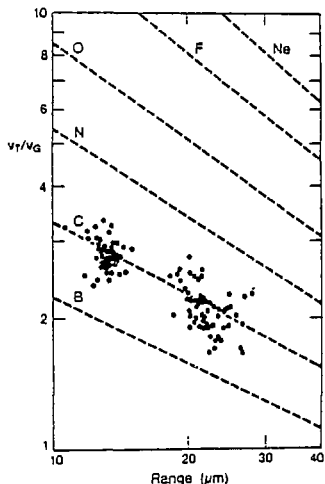

Fig. 10 Ratio of etching rate along track to general etching rate plotted as a function of residual range. Dots represent measurements at two different points along the trajectory of ^{14}C nuclei emitted from ^{223}Ra. Dashed lines are the calibration. From ref. 5.
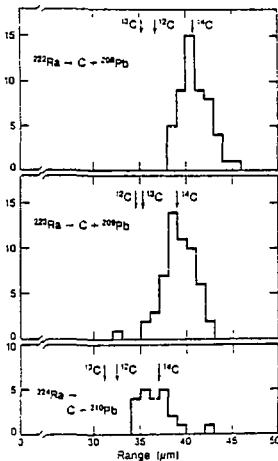

Fig. 11 Results of Price et al.[5] with track detectors and $^{222}, ^{223}, ^{224}Ra$ sources. The histograms are the measured range distributions of ^{14}C compared with ranges calculated from Q-values.

represented by dots whereas calibrations obtained with heavy ions from the LBL Superhilac are given in dashed lines. The location of the dots coincide with the line of C. In figure 11, are compared the histograms of measured ranges with expected ranges corresponding to the Q values of the decays. The agreement in ranges corresponds to an agreement in kinetic energies better than 0.4 MeV.

5.2 – Experiments on decays into Ne fragments

Further experiments at Berkeley[8] and Dubna[10-12] investigated decays into fragments heavier than ^{14}C, using Cronar as a track detector. The following sources were considered : $^{232,233}U$, ^{231}Pa, ^{230}Th, ^{237}Np and ^{241}Am. The common features to all these experiments are related to the very low fragment/α branching ratios which were investigated, i.e. two orders of magnitude lower than in the ^{14}C decay case. Intense sources with extended sizes (in order to keep them relatively thin) and detectors of large area were used. The irradiation time was tens of days. Some data are summarized in table 2. It was found that ^{232}U, ^{231}Pa and ^{230}Th are ^{24}Ne emitters and that ^{233}U is ^{24}Ne or ^{25}Ne emitter.

TABLE 2 : Some characteristics of the experiments with track detectors in the investigation of decays into fragments heavier than ^{14}C.

Decays	Ref.	Strength or mass of the source	Size of the detector (cm^2)	Irrad. time (days)	No of events	Range (μm)	Beams for calibration
$^{232}U \rightarrow ^{24}Ne + ^{208}Pb$	9	0.5mCi	250	30	31	32.9±0.23	^{20}Ne, ^{18}O
$^{231}Pa \rightarrow ^{24}Ne + ^{207}Tl$	10	7 mg	17.5	13	25	30±3	^{20}Ne
$^{233}U \rightarrow ^{24}Ne + ^{209}Pb$	11	75 mg	227	28	16	30.5±1.4	^{20}Ne
$\rightarrow ^{25}Ne + ^{208}Pb$							
$^{230}Th \rightarrow ^{24}Ne + ^{206}Hg$	12	210 mg	1040	64	165	29	$^{16}O, ^{20}Ne, ^{26}Mg$
$^{237}Np \rightarrow ^{20}Mg + ^{207}Tl$	12	320 mg	500	122	0		
$\rightarrow ^{32}Si + ^{205}Au$							
$^{241}Am \rightarrow ^{34}Si + ^{207}Tl$	12	3.7 mg	36	30	0		

The number of observed fragments together with their measured ranges and the beams used for calibration are given in the table. Since no fragments were observed with ^{237}Np and ^{241}Am sources, only upper limits were set for their branching ratios.

With all these findings, the track detector technique appears to be very powerful and incites physicits to search for new decays with still lower branching ratios.

6 - SUMMARY AND DISCUSSION

The different decays into fragments which have been observed or investigated up to now are reported in table 3 with the corresponding experimental and calculated branching ratios relative to α-decays. It is seen that decays of Ra isotopes into ^{14}C occur with Q-values of about 30 MeV and branching ratios of about 10^{-10}, whereas decays of some Th, Pa and U isotopes are characterized by Q-values of about 60 MeV and by branching ratios of about 10^{-12}. All these decays are explained within one order of magnitude by the superasymmetric fission model of references 13 and 14. Better quantitative explanations, however, can be carried out with the same models if hindrance effects for even-odd parents relative to even-even parents are taken into account as it is commonly done in α-decay work. The columns 7 and 8 in table 3 compare the results of branching ratio calculations performed without and with even-odd effects respectively.

Log₁₀ (Bexp/Bth)

221 Ra
222 Ra
223 Ra
224 Ra
225 Ac
225 Ra

230 Th
231 Pa
232 U
233 U
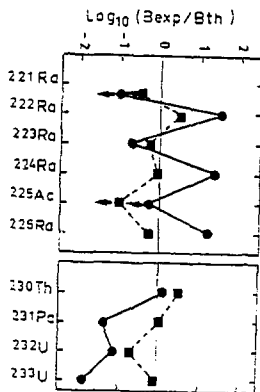
These results are displayed in figure 12 where the full squares corresponding to even-odd effects exhibit, without doubt, an improvement in the explanation of the measured branching ratios.

Other features of the α-decay may also apply here, e. g. the sensitivity of the decay rate to the deformation of the daughter nucleus or the possible transition[6, 17] to excited states in the later.

Fig. 12 Ratioo''nemeasuredtocalculatedbranching ratios displaying the columns 7 and 8 of table 3. In dots, for calculation without even-odd effects and in squares for calculation with even-odd effects.

TABLE 3 :   Decays into fragments observed up to now with their measured and calculated
branching ratios relative to α-decay.

Decay	Q (MeV)	Fragment/α Exp.Branch. Ratio	Ref.	Fragment/α Theor.Br.Ratio Ref.13	Ref.14	$\log_{10}(\frac{Bexp}{Bth})$ (a)	(b)
$^{221}Fr \rightarrow ^{14}C + ^{207}Tl$	31.28	$< 5.0\times10^{-14}$	8	3.2×10^{-12}	7.9×10^{-12}	-0.80	-1.39
$^{221}Ra \rightarrow ^{14}C + ^{207}Pb$	32.39	$< 1.2\times10^{-13}$	8	1.2×10^{-12}	8.2×10^{-12}	-1.02	-0.55
$^{222}Ra \rightarrow ^{14}C + ^{208}Pb$	33.05	$(3.7\pm0.5)10^{-10}$	5	1.0×10^{-11}	1.7×10^{-9}	1.53	0.53
		$(3.1\pm1.0)10^{-10}$	7				
$^{223}Ra \rightarrow ^{14}C + ^{209}Pb$	31.85	$(8.5\pm2.5)10^{-10}$	2	3.2×10^{-9}	6.9×10^{-9}	-0.72	-0.32
		$(5.5\pm2.0)10^{-10}$	3				
		$(7.6\pm3.0)10^{-10}$	4				
		$(6.1\pm0.8)10^{-10}$	5				
		$(4.7\pm1.3)10^{-10}$	6				
$^{224}Ra \rightarrow ^{14}C + ^{210}Pb$	30.54	$(4.3\pm1.1)10^{-11}$	5	1.6×10^{-12}	6.2×10^{-11}	1.43	-0.04
$^{225}Ac \rightarrow ^{14}C + ^{211}Bi$	30.47	$<4.0\times10^{-13}$	8	6.3×10^{-13}	1.6×10^{-12}	-0.20	-0.87
$^{226}Ra \rightarrow ^{14}C + ^{212}Pb$	28.21	$(3.2\pm1.6)10^{-11}$	7	2.0×10^{-12}	3.1×10^{-11}	1.20	-0.23
$^{230}Th \rightarrow ^{24}Ne + ^{206}Hg$	57.78	$(5.6\pm1.0)10^{-13}$	12	4.0×10^{-13}	3.6×10^{-13}	0.15	0.52
$^{231}Pa \rightarrow ^{24}Ne + ^{207}Tl$	60.42	$(4.3\pm0.9)10^{-12}$	10	1.0×10^{-10}	9.4×10^{-12}	-1.37	0.01
$^{232}U \rightarrow ^{24}Ne + ^{208}Pb$	62.31	$(2.0\pm0.5)10^{-12}$	9	1.3×10^{-11}	4.9×10^{-11}	-0.81	-0.41
$^{233}U \rightarrow ^{24}Ne + ^{209}Pb$	60.50	$(7.5\pm2.5)10^{-13}$	11	5.0×10^{-11}	3.7×10^{-11}	-1.82	-0.10
$\rightarrow ^{25}Ne + ^{208}Pb$	60.85			3.2×10^{-11}	2.5×10^{-10}		
$^{237}Np \rightarrow ^{30}Mg + ^{207}Tl$	75.02	$< 4\times10^{-14}$	12	2.5×10^{-12}	2.9×10^{-14}		
$\rightarrow ^{32}Si + ^{205}Au$	88.41			2.5×10^{-12}	3.8×10^{-18}		
$^{241}Am \rightarrow ^{34}Si + ^{207}Tl$	93.84	$< 3\times10^{-12}$	7	4.0×10^{-13}	1.0×10^{-15}		
		$< 3\times10^{-15}$	12				

(a)   Ref. 13

(b)   As in (a) but with even-odd effect accounted for via zero point vibration energy[19].

Let us, also, mention the possible coupling interactions between the fragment and the daughter nucleus during their relative tunneling, by analogy to the ones proposed in the inverse reactions, i.e. the low-energy heavy-ion fusion reactions. Such coupling inducing transfer reaction as well as inelastic excitation could affect the decay rate to the ground state of the daughter and also allow for transitions to final excited configurations[18].

7. CONCLUSION

Several cases of spontaneous emission of fragments from heavy nuclides have been experimentally observed up to now. So, spontaneous decays intermediate between α-decay and fission, previously predicted, are definitively established.

Three experimental techniques have been involved so far giving a striking agreement in branching ratio measurements. The first technique of a ΔExE solid state detector telescope placed in a direct view of the source as in the discovery of the phenomenon seems to have no role left to play. The second technique based on a magnetic selection of the fragments from the very high flux of α-particles is much more powerful in fragment/α branching ratio measurements and present a specific interest in its capability of measuring with precision various characteristics of the fragments, e.g. the energy, Z, A... it is, however, the third technique using track solid detectors which seems to yield the smallest fragment/α branching ratios, and consequently to have in the future the most important role to play.

We have shown that the predictions of the fragment emission were achieved by the use of the traditional models of α-decay and fission. At present, the discovery of several cases of fragment emission and the measurement of their fragment/α branching ratios offer a new field for testing and refining many theoretical aspects involved in α-decay, in fission and even in low-energy heavy-ion fusion.

Finally, it is interesting to point out that many fragment emitters, e.g. ^{223,224,226}Ra, ^{231}Pa and ^{230}Th, occur in the natural series of ^{232}Th or ^{235,238}U. Fragment concentration measurements in U and Th ores should be of interest for applied research.

REFERENCES

1)   A. Sandulescu, D.N. Poenaru and W. Greiner, Sov. J. Part. Nucl. 11 (1980) 528

2)   H.J. Rose and G.A. Jones, Nature 307 (1984) 245

3)   S. Galès, E. Hourani, M. Hussonnois, J.P. Schapira, L. Stab and M. Vergnes, Phys. Rev. Lett. 53 (1984) 759

4)   D.V. Alexandrov, A.F. Belyatsky, Yu. A. Gluhov, E. Yu. Nikol'sky, B.V. Novatsky, A.A. Oglobin and D.N. Stepanov, Pis'ma Zh. Eksp. Teor. Fiz. 40 (1984) 152

5)   P.B. Price, J.D. Stevenson, S.W. Barwick and H.L. Ravn, Phys. Rev. Lett. 54 (1985) 297

6)   W. Kutschera, I. Ahmad, S.G. Armato III, A.M. Friedman, J.E. Gindler, W. Henning, T. Ishii, P. Paul and K.E. Rehm, Phys. Rev. C32 (1985) 2036

7)   E. Hourani, M. Hussonnois, L. Stab, L. Brillard, S. Galès and J.P. Schapira, Phys. Lett. 160B (1985) 375

8)   S.W. Barwick, P.B. Price, H.L. Ravn, E. Hourani and M. Hussonnois (to be published)

9) .   W. Barwick, P.B. Price and J.D. Stevenson, Phys. Rev. C31 (1985) 1984

10)   A. Sandulescu, Yu S. Zamyatin, I.A. Lebedov, B.F. Myasoedov, S.P. Tretyakov and D. Hasegan, JINR Rapid Comm. No 5-84

11)   S.P. Tretyakov, A. Sandulescu, Yu.S. Zamyatin, Yu.S. Korotkin and V.L. Mikheev, JINR Rapid Comm. n° 7-85

12)   S.P. Tretyakova, A. Sandudescu, V.L. Micheev, D. Hasegan, I.A. Lebedev, Yu.S. Zamyatnin, Yu.S. Korotkin and B.F. Myasoedov, JINR Rapid Comm. n°13-85

13)   D.N. Poenaru, M. Ivascu, A. Sandulescu and W. Greiner, J. Phys. G10 (1984) L183 and Phys. Rev. C32 (1985) 572

14)   Yi-Jin Shi and W.J. Swiatecki, Phys. Rev. Lett. 54 (1985) 300 and Nucl. Phys. A438 (1985) 450

15)   J.P. Schapira, F. Azaiez, S. Fortier, S. Galès, E. Hourani, J. Kumpulainen and J.M. Maison, Nucl. Instr. and Meth. 224 (1984) 337

16)   R.L. Fleischer, P.B. Price and R.M. Walker, Nuclear Tracks in Solids : Principles and Applications (Univ. of California Press, Berkeley, 1975)

17)   M. Greiner and W. Scheid (private communication)

18)   S. Landowne and C.H. Dasso, Phys. Rev. C33 (1986) 387

19)   D.N. Poenaru, M. Ivascu, W. Greiner, D. Mazilu, I.H. Plonski (to be published)